Influence of fluorspar replacement in desulfurizing mixtures and variation of process parameters on the hot metal desulfurization efficiency

http://dx.doi.org/10.1590/0370-44672023760021

Flaviani M. Marchesi[1,4]
https://orcid.org/0000-0003-0325-9491
Estéfano Aparecido Vieira[1,5]
https://orcid.org/0000-0003-2131-6920
Jean C. D. de Paola[2,6]
https://orcid.org/0000-0002-6675-7618
Eduardo Junca[3,7]
https://orcid.org/0000-0002-7068-2583
Felipe Fardin Grillo[1,8]
https://orcid.org/0000-0002-0224-9075
José Roberto Oliveira[1,9]
https://orcid.org/0000-0003-3785-2306

[1]Instituto Federal de Educação Ciência
e Tecnologia do Espírito Santo - IFES,
Departamento de Engenharia Metalúrgica,
Vitória – Espírito Santo - Brasil.

[2]Universidade Cidade de São Paulo – UNICID,
Departamento de Engenharia Elétrica,
São Paulo – São Paulo - Brasil.

[3]Universidade do Extremo Sul Catarinense - UNESC,
Programa de Pós-Graduação em Ciência e Engenharia
de Materiais, Criciúma - Santa Catarina - Brasil.

E-mails: [4]vianimarchesi@hotmail.com,
[5]estefanovieira@ifes.edu.br, [6]jean.depaola@alumni.usp.br,
[7]eduardojunca@unesc.net, [8]felipe.grillo@ifes.edu.br,
[9]jroberto@ifes.edu.br

Abstract

Fluorspar (CaF_2) is the most used flux in hot metal desulfurizing mixtures. However, its use can cause refractory wear and environmental contamination, prompting research efforts to develop alternative desulfurizing mixtures. This study aims to investigate the replacement desulfurizing mixtures containing fluorspar by other desulfurizing mixtures containing a new flux developed without fluorspar named MIX. The influence of varying the mass of these desulfurizing mixtures, temperature, and stirring of the system on the efficiency of hot metal desulfurization was also studied. The desulfurization experiments were carried out in an electric resistance furnace, at a temperature of 1370°C. Hot metal samples were taken to measure the change in sulfur content in the experiments. FactSage 8.0 software, was used to determine the phases present in the desulfurizing mixtures, and these phases were correlated with the hot metal desulfurization efficiency. The efficiency of the desulfurizing mixtures was also correlated with the Desulfurization Factor. The results showed that desulfurizing mixtures containing fluorspar are the most efficient mixtures. However, fluorspar-free desulfurizing mixtures containing MIX can achieve similar efficiencies with increases in mass, temperature, and system stirring. The results also showed that the most efficient desulfurizing mixtures are those with higher percentages of solid CaO and lower percentages of the solid phases $3CaO.SiO_2$ and CaS and, consequently, a higher Desulfurization Factor.

Keywords: hot metal, desulfurization, fluorspar replacement, desulfurization factor.

1. Introduction

The use of fluorspar as a flux in desulfurizing mixtures is widespread in steelmaking industries, and in certain proportions, prevents the formation of solid phases around the lime particle, impairing the mass transport of sulfur to this particle, and consequently, impairing the desulphurization reaction that occurs in accordance with Equation (1) (Pezzin *et al.*, 2020; Santos *et al.*, 2021; McFeaters & Fruehan, 1993). However, due to their use causing wear and tear on refractories and environmental contamination (Choi *et al.*, 2001), these industries are looking to replace it (Yang *et al.*, 2007; Niedringhaus *et al.*, 1988; Mitsuo *et al.*, 1982) with alternative fluxes. Hot metal desulfurization is usually represented by Equation 1. For the levels of silicon contained of hot metal, the oxygen released by Equation 1 can react with these elements, according to Equation 2.

$$[S] + CaO_s \rightarrow CaS_s + [O] \qquad \Delta G^0 = 115358 - 38.66.T\,[J/mol] \qquad (1)$$

$$2CaO_s + [S] + 1/2\,[Si] \rightarrow CaS_s + 1/2\ Ca_2SiO_{4s} \qquad \Delta G^0 = -246222 + 78T\,[J/mol] \qquad (2)$$

This reaction shows that the hot metal desulfurization process is exothermic, so an increase in temperature causes an increase in the metal sulfur content in the reaction equilibrium between hot metal and the desulfurizing mixtures.

Several authors state that the improvement in desulfurization efficiency when adding fluorspar or another flux is due to the reduction of the solid phases ($3CaO.SiO_2$) and ($3CaO.Al_2O_3$) that form around the lime particle and impair the desulfurization process (Santos *et al.* 2021; McFeaters & Fruehan, 1993; Choi *et al.*, 2001; Yang *et al.*, 2007; Mitsuo *et al.*, 1982; Grillo *et al.*, 2016; Lindström & Sichen, 2015). Niedringhaus & Fruehan (1988) state that the increase in temperature also has this effect. According to the authors, in the case of the KR process, which is the process researched in this study, the desulfurization occurs through the contact of sulfur with solid CaO. Choi *et al.* (2001) proposed the model represented by Equation 3, to evaluate the kinetics of the hot metal desulfurization reaction.

$$-\frac{d[\%S]}{dt} = K'.\left(\frac{A}{V_m}\right).\{[\%S_t] - [\%S_{eq}]\} \qquad (3)$$

Where: k' is the global sulfur mass transfer coefficient (m/s); A is the Interfacial Area between hot metal and lime particles (m^2) and V_m = Metal volume (m^3). S_t = sulfur concentration in steel at time t; S_{eq} = sulfur concentration in hot metal in equilibrium between hot metal and desulfurizing mixtures.

However, according to Nakai *et. al.* (2010) , due to the difficulty of determining some parameters, Equation 3 can be reduced to Equation 4:

$$\frac{d[\%S]}{dt} = -K([\%S_t] - [\%S_{eq}]) \qquad (4)$$

Where: $K = k'.(A/V_m)$ is the velocity constant (min^{-1} or s^{-1}). K is a function of the mass transport of sulfur in the metal and slag.

Nakai *et. al.* (2010) developed a model to calculate the stirring energy of hot metal caused by impeller rotation in the desulfurization process via KR and related this energy to the velocity constant. Santos *et al.* (2021). On the other hand, by analyzing simulations performed with FactSage, they related the solid and liquid phases present in the hot metal desulfurizing mixtures with the experimental results. The author presented a parameter called Desulfurization Factor (FDeS), which estimates the desulfurization efficiency by an equation with a relationship between the amount of solid CaO (free lime) and the solid phases that hinder desulfurization. These phases were calculated by thermodynamic simulations of the desulfurizing mixtures using the software FactSage. FDeS is presented in Equation 5, and in the experiments of the referred to author, the coefficient of determination between FDeS and the desulfurization efficiency was about 0.990.

$$FDeS = (\%CaO_s) - (\%\ 3CaO.SiO_{2(s)} + \%\ 3CaO.Al_2\,O_{3(s)} + \%\ (\%CaS_s) \qquad (5)$$

Based on these results, Santos *et al.* (2021) states that the higher the FDeS, the higher the desulfurization efficiency. However, the relationship between these variables (Eq. 5) and the results of correlation with the desulfurization efficiency, described by the FDeS, are only valid for situations where there is no variation in process parameters, such as temperature, stirring, lime granulometry and reactivity (parameters that affect the process kinetics). FactSage is a thermodynamic simulation software, so these kinetics parameters are not considered in the results. In other words, FDeS evaluates the desulfurization efficiency for different desulfurizing mixture compositions. It effectively evaluates the phases that will be formed with the different compositions, and through the phases formed, it evaluates the efficiency of the desulfurizing mixtures. In other words, what matters in a hot metal desulfurization with lime-based desulfurizing mixtures are the phases that are formed around the lime particle during the reaction. The composition of the desulfurizing mixtures is only a means of obtaining the best phase ratio, according to Santos *et al.* (2021).

Thus, this article studies the replacement of desulfurizing mixtures containing fluorspar by other desulfurizing mixtures containing a new flux developed without fluorspar named MIX, including the influence of varying the mass of these desulfurizing mixtures, temperature, and stirring of the system on the hot metal desulfurization efficiency. FactSage was used to determine the phases present in the desulfurizing mixtures, and these phases were correlated with the desulfurization efficiency of the desulfurizing mixtures. The efficiency of the desulfurizing mixtures was also correlated with the Desulfurization Factor parameter.

2. Materials and methods

The chemical composition of hot metal used can be seen in Table 1. Table 2 shows the chemical composition of the raw materials used.

Table 1 - Chemical composition of hot metal used in the experiments.

% Fe	% C	% Si	% Mn	% P	% S
94.2	4.5	0.27	0.17	0.08	0.06

Table 2 - Chemical composition of the reagents used in the desulfurization tests.

	Al	Al_2O_3	CaO	K_2O	Na_2O	S	SiO_2	CaF_2
Lime 0-2mm	0.00	0.27	98.16	0.00	0.00	0.12	1.45	0.00
MIX*	15.84	22.84	3.88	3.12	26.92	0.03	27.36	0.00
Fluorspar	0.00	2.48	3.70	0.00	0.00	0.02	2.55	91.24

*A new alternative fluorspar free flux developed named MIX.

An alternative fluorspar free flux, called MIX, was used to replace the fluorspar desulfurizing mixtures. The desulfurizing mixtures were composed of lime and a flux. In Table 3, the "desulfurizing mixtures mass" is the total mass of added mixture to desulfurization, the "%Flux" presents the mass percent of flux (MIX or fluorspar) in the total mass and the remaining amount in the mixtures is lime. In the alternative mixture, the fluxes were Al_2O_3, K_2O and Na_2O instead of fluorspar. These compounds were added to MIX as analytical standards with purity greater than 99%. Table 3 shows the proposed comparison of the following parameters between experiments: variation of fluxes, mass variation, temperature and stirring. The particle size range is the same for all experiments and all materials (0-2 mm), as well as the impeller rotation (500 rpm). The chemical composition of the desulfurizing mixtures is shown in Table 4.

Table 3 - Experimental conditions for experiments grouped by different comparison objects.

Test	Desulfurizing mixtures mass (g)	% Flux**	Desulfurizing mixtures	Temperature (°C)	Impeller	Comparison Object
Exp 2	6.5	12	MIX	1370	1	Different fluxes
Exp 6	6.5	10	With Fluorspar	1370	1	
Exp 3	8	12	MIX	1370	1	Desulfurizing Mixture Mass
Exp 1	7	12	MIX	1370	1	
Exp 2	6.5	12	MIX	1370	1	
Exp 7	7	12	MIX	1320	1	Temperature
Exp 1	7	12	MIX	1370	1	
Exp8	7	12	MIX	1420	1	
Exp 1	7	12	MIX	1370	1	Stirring Energy
Exp 9	7	12	MIX	1370	2	

** The rest is lime.

Table 4 - Chemical composition of the desulfurizing mixtures.

Experiment number	Chemical Composition (%)							
	Al	Al_2O_3	CaO	K_2O	Na_2O	S	SiO_2	CaF_2
1, 3, 7, 8, 2, 9	2.08	3.18	85.91	0.44	3.48	0.11	4.79	0.00
6	0.00	0.53	88.07	0.00	0.00	0.11	1.79	9.61

The experiments were carried out to simulate the KR process, where the desulphurizing mixture is added to the ladle containing the liquid hot metal and the system is stirred by an impeller according to Figure 1. For carrying out the experiments, MgO-C crucibles were used to melt 1 kg of hot metal per experiment. The experiments were carried out in an argon atmosphere at a flow rate of approximately 4 NL/min. The argon injection was started with the addition of hot metal and remained throughout the experiments. Once the working temperature was reached, 1400°C, the complete melting of the hot metal was verified by means of a secondary inlet, and an initial sample was taken through a vacuum quartz sampler (for initial sulfur analysis) and then the additions of desulfurizing materials. To assist with additions, a stainless-steel tube was used to direct the material into the crucible. Figure 1 shows a scheme for taking samples during experimental tests.

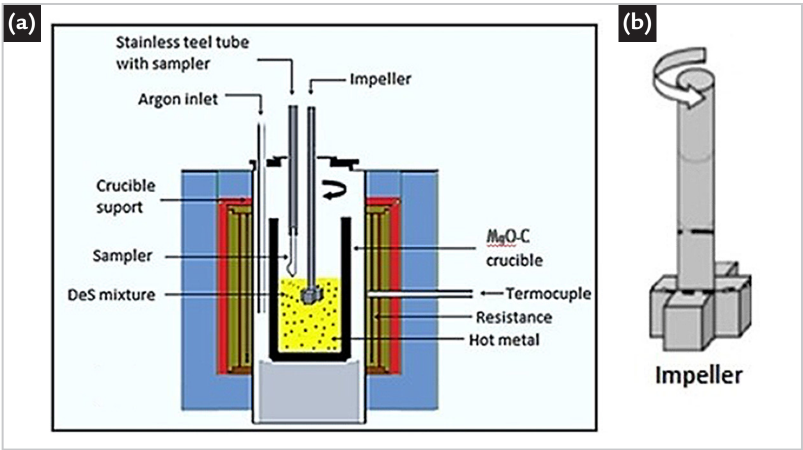

Figure 1 - (a) Schematic diagram of the experiments performed; (b) Impeller.

After adding the desulfurizing mixtures, the mechanical stirrer was started with the propeller rotating at 500 rpm. The reaction time started to be counted immediately after the slag was loaded. Samples were taken before the additions and at 2, 5, 8, 12, 15 and 20 minutes after the additions. This procedure is performed through an opening located in the center of the furnace lid, using vacuum samplers. Each sample weighed approximately 10 grams.

Using the composition of the hot metal and the desulfurizing mixtures , the equilibrium sulfur content was determined in each experiment using FactSage. The properties of the desulfurizing mixtures (percentage of solids and liquids and as phases present) were also determined using FactSage. The system stirring energy was calculated according to models proposed in literature (Nakai *et al.*, 2010) and the efficiency of the desulfurization process (η) was calculated based on the initial and final values of sulfur present in the metal by Equation 6.

$$\eta\ (\%) = \frac{[S]_{initial} - [S]_{last}}{[S]_{initial}} \times 100 \qquad (6)$$

3. Results and discussion

3.1 Influence of the variation of the addition of the different fluxes

In order to evaluate a possible replacement of the desulfurizing mixtures containing fluorspar by another desulfurizing mixture containing a new flux developed without fluorspar named MIX, the following desulfurizing mixtures were proposed. Table 5 shows the phases present in the desulfurizing mixtures S at 1370⁰C determined by FactSage to evaluate the influence of varying the desulfurizing mixtures.

Table 5 - Phases present at 1370⁰C determined by FactSage in the desulfurizing mixtures with different fluxes.

Desulfurizing mixtures	Solid Phases (%)				Solids (%)	Liquid (%)	$\%S_{eq}$	η (%)	FDeS
	CaO	Ca_3SiO_5	CaS	MgO					
Exp 2	65.9	12.29	0.3	0	78.43	21.57	3.62E-05	37.2	53.36
Exp 6	83.6	0	0.2	0	83.79	16.21	2.93E-05	70.30	83.36

It can be seen from the data in Table 5, that the desulfurizing mixtures containing fluorspar had the highest percentage of solid CaO and the least amount of the solid phases that form around the lime particles. Because of this, it had the highest FDeS and the highest desulfurization efficiency. Table 6 shows the variation of the S content with time, and Figure 2 the variation of the $\%S/S_0$ ratio over the various times of the experiment.

Table 6 - Sulfur variation with sampling time to evaluate flux variation.

Desulfurizing mixtures	Time(min)						
	0	2	5	8	12	15	20
Exp 6	0.051	0.042	0.027	0.025	0.018	0.016	0.015
Exp 2	0.053	0.049	0.049	0.048	0.042	0.042	0.033

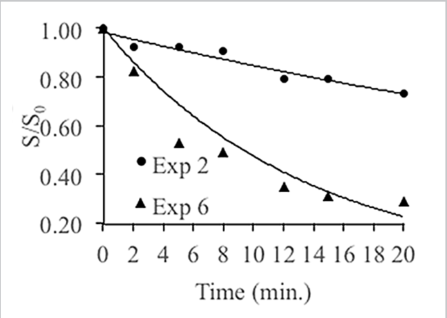

Figure 2 - Variation of $\%S/S_0$ as a function of the time to evaluate the influence of different fluxes.

It can be seen from Table 6 that the use of the proposed desulfurizing mixtures decreases the sulfur present in hot metal. Notice that in Table 6 and Figure 2, Experiment 6, obtained a lower final sulfur level (0.015 versus 0.033% of desulfurizing mixture 2), and consequently, a higher desulfurization efficiency (70.30% versus 37.2%). Furthermore, after 5 minutes of reaction, Experiment 6 already showed a 46.0% desulfurization efficiency ($\%S_{initial} = 0.051$ and %S at 5 minutes, 0.027%), which is a 12.25% higher efficiency over the entire experiment time when compared to the Experiment 2. This occurred because, according to Table 5, in the case of using the desulfurizing mixture with MIX in the Experiment 2, approximately 12% of $3CaO.SiO_2$ was formed. So, the thermodynamic simulation result in Table 5 indicates the formation of about 12% of $3CaO.SiO_2$ in the mixture containing MIX (Experiment 2), which is not a guarantee, but supports an explanation for the efficiency difference and sulfur removal profile that can be seen in Figure 2. This phase is formed by the reaction of SiO_2 with CaO, consuming the CaO that could react with sulfur, and forming a layer of solid around the CaO particle, making it difficult to transport the sulfur mass into the solid CaO.Therefore, the formation of $3CaO.SiO_2$ decreases the metal-CaO interface area (term A of Equation 3) and the sulfur mass transport slows down, and consequently, the efficiency of the process. In other words, as the solid phases decrease, the desulfurization efficiency increases. These results agree with those obtained from literature (Santos *et al.* 2021; McFeaters & Fruehan, 1993; Choi *et al.*, 2001; Yang *et al.*, 2007; Mitsuo *et al.*, 1982; Grillo *et al.*, 2016; Lindström & Sichen, 2015). This shows that fluorspar is a more efficient flux than those used in these desulfurizing mixtures. Analyzing the FDeS values for the experiments presented in Table 5, the values for tests 1, 3, and 2 are the same because there was no variation in the composition of the slag.

It can also be noted that the higher the FDeS, the higher the desulfurization efficiency. The FDeS shows that the most efficient desulfurizing mixtures will be the one that has no solid phase formed around the CaO particle. In this case, the maximum theoretical value of FDeS would be 100. But in practice this is unlikely to be achieved, since to eliminate these phases, it is necessary to add fluxes, which also leave part of the liquid CaO.

3.2 Influence of mass variation

Experiments 1 and 2 aimed to verify the influence of varying the amount of lime mass. Table 7 shows the results of the simulations performed in FactSage for the desulfurizing mixtures, to evaluate the influence of varying the mass.

Table 7 - Phases present at 1370 C determined by FactSage in the desulfurizing mixtures with different mass.

Desulfurizing mixtures	Solid Phases (%)				Solids (%)	Liquid (%)	$\%S_{eq}$	Mass (g)	η (%)
	CaO	Ca_3SiO_5	CaS	MgO					
Exp 3	65.5	12.60	0.3	0	78.72	21.22	3.61E-05	8	60.4
Exp 1	65.6	12.62	0.3	0	78.72	21.28	3.61E-05	7	40.98
Exp 2	65.6	12.62	0.3	0	78.7	21.30	3.61E-05	6.5	37.2

It can be seen from the data in Table 7 that the phases present and the Seq content of the three desulfurizing mixtures presented the same values, so this difference in mass was not relevant to modify the equilibrium sulfur content. This was expected, because the mass of the desulfurizing mixtures does not change the properties shown in Table 7, since the composition was the same. Table 8 shows the variation of the S content with time, and Figure 3 shows the variation of the $\%S/S_0$ ratio with time.

Table 8 - Sulfur variation with sampling time to evaluate the influence of mass variation.

Desulfurizing mixtures	%S						
	0	2	5	8	12	15	20
Exp 1	0.061	0.052	0.058	0.05	0.045	0.042	0.036
Exp 3	0.061	0.05	0.043	0.04	0.037	0.032	0.029
Exp 2	0.053	0.049	0.049	0.048	0.042	0.042	0.033

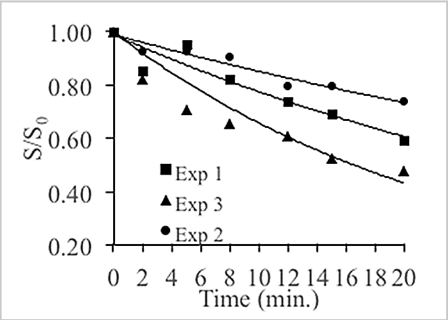

Figure 3 - Variation of sulfur S/S_0 as a function of the time to evaluate the influence of mass variation.

Figure 3 shows that the desulfurizing mixtures with higher masses presented a higher sulfur removal, and consequently, higher desulfurization efficiency. This increase occurs because the greater the amount of desulfurizing mixture mass, the greater the metal-CaO interface area (term A of Equation 3), improving the kinetics of the process according to Equation 3, and consequently, the efficiency of the process.

It can also be seen that an increase in desulfurizing mixture mass from 6.5 grams to 8 grams increased the desulfurization efficiency from 37.2 to 60.4 %, or a 38.4% increase. This is an indication that although fluorspar is a more efficient fluxing agent, similar desulfurization efficiencies can be achieved with the flux MIX desulfurizing mixture proposed in this article, using a larger desulfurizing mixture mass. Even using larger mass, this replacement may be feasible. This is because the MIX mixture might not cause the environmental problems and the refractory wear that fluorspar causes, due to lower K_2O and Na_2O contents (respectively 3.88 e 26.92%) compared to the CaF_2 content (91.24%).

3.3 Influence of temperature variation

Experiments 1, 7 and 8 aimed to evaluate the temperature variation with a range of 50 °C above and below the base temperature, 1370 °C. Table 9 presents the results of the simulations of the initial desulfurizing mixtures obtained by the FactSage.

Table 9 - Phases present at 1370 ^{0}C determined by FactSage in the desulfurizing mixtures with different temperatures.

Desulfurizing mixtures	Solid Phases (%)				Solids	Liquid (%)	T (^{0}C)	%S_{eq}	η (%)	FDeS
	CaO	Ca_3SiO_5	CaS	MgO						
Exp7	65.3	15.24	0.3	0	80.81	19.19	1320	1.89E-05	30.61	49.76
Exp 1	65.7	12.72	0.3	0	78.72	21.28	1370	3.61E-05	40.98	52.68
Exp 8	66.6	8.32	0.3	0	75.2	24.8	1420	6.58E-05	56.1	57.98

Table 9 demonstrates that an increase in temperature entails an increase in the equilibrium sulfur value (1320 °C Experiment 7 = 1.889E-05 < 1370 °C Experiment 1 = 3.611E-05 < 1420 °C Experiment 8 = 6.580E-05). This is because in hot metal desulfurization with the presence of silicon, the sulfur removal reaction occurs according to Equation 7 (G°= -492444+ 156.T, in J/mol), which is exothermic. An increase in temperature will increase the equilibrium sulfur content.

$$4CaO_{(s)} + \underline{2S} + \underline{Si} \rightarrow 2CaS_{(s)} + Ca_2SiO_{4(s)} \qquad (7)$$

This sulfur content equilibrium (less than 1ppm) is irrelevant as far as kinetics is concerned, based on Equation 3. However, the data in Table 9, show that there is a reduction in the number of solid phases formed and a higher percentage of liquid with increasing temperature. Thus, the improvement in the sulfur removal process occurs due to the kinetic improvement of the process by reducing the solid phases and increasing the presence of the liquid phase. Table 10 shows the variation of the S content with time, and Figure 4, the variation of the $\%S/S_0$ ratio with time. Figure 4 shows the values of the sulfur variation over time for the experiments with temperature variation.

Table 10 - Sulfur variation with sampling time to evaluate the influence of temperature.

Desulfurizing mixtures	%S						
	0	2	5	8	12	15	20
Exp 1	0.061	0.052	0.058	0.05	0.045	0.042	0.036
Exp 7	0.049	0.048	0.046	0.047	0.042	0.044	0.034
Exp 8	0.041	0.038	0.028	0.026	0.022	0.019	0.018

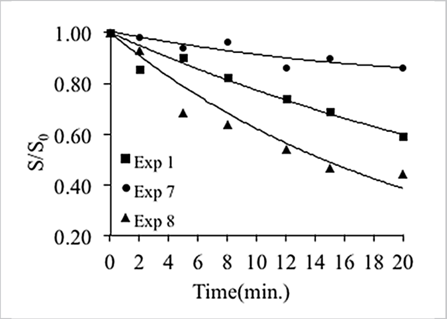

Figure 4 - Variation of sulfur S/S_0 as a function of the time to evaluate the influence of temperature variation.

In Figure 4 and Table 10, the highest temperature at which Experiment 8 occurred (1420°C) provided a lower final sulfur content of 0.018% and 56.1% desulfurization efficiency. Then, Experiment 1 (1370 °C) obtained 0.0360 final sulfur and 40.98% efficiency, while Experiment 7, the lowest temperature among these experiments (1320 °C), values were 0.034 and 30.61 % sulfur removal.

That is, a 50-degree increase in temperature caused a 36.8% increase in desulfurization efficiency. As with the increase in desulfurizing mixture mass, this is an indication that even though fluorspar is a more efficient flux, a similar desulfurization efficiency can be achieved with the MIX desulfurizing mixture, using a higher process temperature.

As shown earlier, it can be seen from the Table 3 that the temperature increase raises the value of the equilibrium sulfur, since the hot metal desulfurization reaction is exothermic, as shown in Equation (2). However, experimental results show that an increase in temperature causes an increase in process efficiency.

This occurs because, according to Table 9, there is a reduction in the number of solid phases formed and a higher percentage of liquids. Thus, the improvement in the sulfur removal process occurs due to the kinetic improvement of the process, through the reduction of the calcium silicates formed, and the presence of a larger liquid phase.

When analysing the values of the Desulfurization Factor shown in Table 9, it can be seen that the higher the value, the greater the desulfurization efficiency. This shows that, although the Desulfurization Factor is a parameter designed to evaluate the desulfurization efficiency as a function of desulfurizing mixture composition, in the present study it can also be used to evaluate desulfurization efficiency as a function the temperature change, as far as the temperature change affects the phase equilibria.

3.4 Influence of stirring energy system

To study the influence of the stirring energy, Experiment 1 was repeated using a different impeller. The results show that the desulfurization efficiency found in Experiment 1 was 40.98%.

This efficiency is considered low for industrial hot metal desulfurization processes via KR. The efficiency values considered good in industrial processes are greater than 70%. However, the industry normally uses 5 kg of desulfurizing mixture per metric ton of hot metal, for every 0.03% of sulfur present in the hot metal.

The low efficiency of sulfur removal, shown in Experiment 1, occurred because the desulfurizing mixture used was 7 kg/t. This mass was used because it was assumed that the hot metal had 0.03 % of sulfur. However, the starting sulfur was 0.061%, and for these levels, industrially, 11 to 13 kg of desulfurizing mixtures are used per metric ton of hot metal (according to information provided by the company). In addition, the stirring energy used was 0.050W. The stirring energy in the KR system can be calculated using Equation 8, proposed by Nakai *et al.*, 2010.

$$P = Np.\rho.n^3.d^5 \tag{8}$$

To study the influence of the stirring energy, 2 different impellers were used with the process characteristics described in Table 11. From the data presented in Table 11, it was possible to calculate the stirring energy by mechanical stirring proposed by Nakai *et al.* (2010).

Table 11 - Parameters used in the calculation of the stirring energy (Nakai *et al.*, 2010).

	Symbol	**Unity**	**Impeller 1**	**Impeller 2**
Impeller Height	b	m	0.01	0.043
Average ladle diameter	D	m	0.07	0.07
Height of the liquid column in the ladle	Z	m	0.031	0.09
Density	ρ	kg/m^3	6300	7000
Rotation speed	n	1/s	6.667	8.333
Impeller diameter	d	m	0.03	0.04
Steel viscosity	μ	Pa.s	0.006	0.007
Rotation speed	N	RPM	400	500
Typical hot metal weight	Q	t	0.00075	0.00242

The impeller format used is the same as shown in Figure 1b. And it has the same format as the impeller used industrially.From the data presented, it was possible to calculate the stirring energy by mechanical stirring proposed by Nakai *et al*. (Equation 8). The parameters needed for the calculation are shown in Table 12.

Table 12 - Stirring energy and specific stirring energy for the KR and impeller data used in this study.

Formulas	**Impeller 1**	**Impeller 2**	**Unity**
$Re = \rho.n.d^2/ \mu$	6300	13333	
$p = 1.1+4.(2b/D)-2.5.(d/D-0.5)^2-7.(2b/D)^4$	2.18	-9.95	
$B = 10^{**} \{1.3-4.(2b/D-0.5)^2-1.14.(d/D)\}$	4.24	0.03	
$a = 14+(2b/D).\{670.(d/D-0.6)^2+185\}$	72.48	241.96	
$Np = a/Re + B.[(10^3+1.2Re^{0.66}) / (10^3+3.2Re^{0.66})] . (Z/D)^{**}(0.35+2b/D)$	1.11	7.11	
$P = Np. \rho.n^3.d^5$	0.050	2.951	W
P	0.000050	0.0029507	kW
P specific	0.067	1.217	kW/t

Where: Re: Reynolds coefficient, Np: power number (-), P: stirring energy (W), a, B, P: proportional constant (-).

From the data presented, to evaluate the influence of stirring on the desulfurization process, it was proposed to perform 2 experiments with the desulfurizing mixture referring to Experiment 1 (7kg CaO/t of desulfurizing mixture with 12% MIX using different impellers.

Table 13 - shows the variation of S content with time, and Figure 5 the variation of %S/S_0 ratio with time.

Stirring	**%S**						
	0	**2**	**5**	**8**	**12**	**15**	**20**
Impeller 1	0.053	0.049	0.049	0.048	0.042	0.042	0.039
Impeller 2	0.054	0.048	0.049	0.048	0.049	0.046	0.043

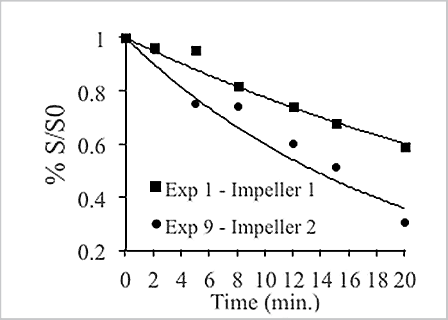

Figure 5 - Variation of sulfur S/S_0 as a function of time to evaluate the influence of stirring.

According to the experiments, the use of an impeller with higher stirring energy (Experiment 1 - impeller 2) provided a higher level of sulfur removal when compared to Experiment 1 - impeller 1 with its final sulfur values in percentages of 0.01 and 0.036, respectively. Table 14 shows the influence of stirring energy on the efficiency of the process.

Note that Experiment 1- impeller 2 obtained an efficiency of 69.70%. This occurs because higher stirring energy of the system causes a higher mass transport coefficient of sulfur, and according to Equation 3 increases the process stirring, and consequently, the efficiency.

Table 14 - Influence of stirring energy on the efficiency of the process.

Parameters	Impeller 1	Impeller 2	Unity
P	0.0000504	0.0029507	kW
P specific	0.067	1.217	kW/t
η	40.98	69.7	%

Like the mass and temperature increase experiments, this result is an indication that although fluorspar is a more efficient flux, a similar desulfurization efficiency can be achieved with the MIX desulfurizing mixture using a higher bath stirring energy.

4. Conclusions

For the conditions analyzed in the present study, it can be concluded that:

1. The highest desulfurization efficiency was obtained using Fluorspar, reaching values of 0.0130% S and 74% desulfurization efficiency. Therefore, Fluorspar is the most efficient flux.

2. An increase in the mass of the mixtures, increased the sulfur removal, and consequently increased the efficiency in the desulfurization process, because the greater the amount of mass of the desulfurizing mixture, the greater is the area of the metal-CaO interface, improving the kinetics of the process, and consequently, the efficiency of the process. An increase in the desulfurizing mixture mass from 6.5 to 8g increased the desulfurization efficiency from 37.2 to 60.4 %, i.e., an increase of 38.4%.

3. Increasing the temperature increases the efficiency of desulfurization, even harming the thermodynamic conditions (of the hot metal, which has silicon in its composition). This is because the reduction of solid compounds formed improves the kinetics to such an extent that it compensates for this. A 50 degree increase in temperature caused an increase in desulfurization efficiency of 36.8%.

4. The stirring energy provided by rotor 2 was more efficient than rotor 1, with an efficiency of 69.7 versus 40.98 respectively; a 41.2% increase.

5. The most efficient desulfurizing mixtures are those that produce a higher percentage of solid CaO and lower percentage of the solid phases $3CaOSiO_2$ and CaS, and consequently, a higher Desulfurization Factor.

6. The desulfurization factor can be used to evaluate the desulfurization efficiency as a function of the composition.

7. Even though desulfurizing mixture with fluorspar is the most efficient desulfurizing mixture, similar desulfurization efficiencies can be obtained with desulfurizing mixture containing the flux MIX, by using a larger mass of that mixture, at higher temperatures and with greater stirring. Thus, a replacement of fluorspar with one of the proposed mixtures may become feasible, since the flux MIX does not cause the environmental problems, nor the refractory wear that fluorspar causes.

Acknowledgments

Thanks to CAPES, FAPES and CNPq for funding research grants and IFES - Campus Vitória for the equipment and specialized knowledge.

References

CHOI, J.; KIM, D.; LEE, H. Reaction kinetics of desulfurization of molten pig iron using $CaO–SiO_2–Al_2O_3–Na_2O$ slag systems. ***ISIJ International,*** v. 41, p. 216-224, 2001.

GRILLO, F. F.; COLETI, J. L.; OLIVEIRA, J. R.; TENÓRIO, J. A. S.; JUNCA, E.; ESPINOSA, D. C. R. Use of computational thermodynamics in the analysis of hot metal desulphurization with slags based on marble waste and sodalite. ***Materials Transactions,*** v. 58, p. 1332-1338, 2016. DOI: https://doi.org/10.2320/matertrans.M2016016.

LINDSTRÖM, D.; SICHEN, D. Study on desulfurization abilities of some commonly used desulfurization agents. ***Steel Research International,*** v. 86, p.73-83, 2015. DOI: https://doi.org/10.1002/srin.201400031.

MCFEATERS, L. B.; FRUEHAN, R. J. Desulfurization of bath smelter metal. ***Metallurgical and Materials Transactions B,*** v. 24B, p. 441-447, 1993.

MITSUO, T.; SHOJI, T.; HATTA, Y.; ONO, H.; MORI, H.; KAI, T. Improvement of desulfurization by addition of aluminum to hot metal in the lime injection process. ***Transactions of the Japan Institute of Metals,*** v. 23, n. 12, p. 768-779, 1982. DOI: https://doi.org/10.2320/matertrans1960.23.768.

NAKAI, Y.; SUMI, I.; MATSUNO, H.; KIKUCHI, N.; KISHIMOTO, Y. Effect of flux dispersion behavior on desulfurization of hot metal. ***ISIJ International,*** v. 50, n. 3, p. 403-410, 2010. DOI: https://doi.org/10.2355/isijinternational.50.403.

NIEDRINGHAUS, J. C.; FRUEHAN, R. J. Reaction mechanism for the CaO-Al and $CaO-CaF_2$ desulfurization of carbon--saturated iron. ***Metallurgical Transactions B,*** v. 19B, p. 261-268, 1988. DOI: https://doi.org/10.1007/BF02654211.

PEZZIN, Rodrigo de Oliveira; BERGER, Anna Paula Littig; GRILLO, Felipe Fardin; JUNCA, Eduardo; FURTADO, Henrique Silva; OLIVEIRA, José Roberto de. Analysis of the influence of the solid and liquid phases on steel desulfurization with slags from the $CaO-Al_2O_3$ systems using computational thermodynamics. ***Journal of Materials Research and Technology - JMR&T,*** v. 9, p. 838-846, 2020. DOI: https://doi.org/10.1016/j.jmrt.2019.11.023.

SANTOS, E. V. E.; OLIVEIRA, S. M. R. D.; SILVA, C. V.; GRILLO, F. F.; OLIVEIRA, J. R. Development of a new parameter for predicting hot metal desulfurization efficiency. ***REM - Int. Eng. J.,*** v. 74, p. 443-450, 2021. DOI: https://doi.org/10.1590/0370-44672021740001.

SANTOS, E. V. E.; SOARES, S. G.; OLIVEIRA, H. C. C.; JUNCA, E.; GRILLO, F. F.; OLIVEIRA, J. R. Influence of industrial wastes and different fluxes on hot metal desulfurization efficiency. ***JOM,*** p. 1909-1918, 2021. DOI: https://doi.org/10.1007/s11837-021-04673-3.

YANG, J.; KUWABARA, M.; ASANO, T.; CHUMA, A.; DU, J. Effect of lime particle size on melting behavior of lime--containing flux. ***ISIJ International,*** p. 1401-1408, 2007. DOI: https://doi.org/10.2355/isijinternational.47.1401.

Received: 27 February 2022 - Accepted: 1 May 2023.